Sex-specific resilience of neocortex to food restriction

Zahid Padamsey[1,2,4], Danai Katsanevaki[2,3], Patricia Maeso[2], Manuela Rizzi[2], Emily Osterweil[2,3] and Nathalie L. Rochefort[2, 3, 4]

[1] Wellcome-MRC Institute of Metabolic Science, University of Cambridge, CB2 0QQ, Cambridge, United Kingdom.

[2] Centre for Discovery Brain Sciences, School of Biomedical Sciences, University of Edinburgh, EH8 9XD, Edinburgh, United Kingdom.

[3]Simons Initiative for the Developing Brain, University of Edinburgh, EH8 9XD, Edinburgh, United Kingdom.

[4]corresponding authors: zp278@cam.ac.uk, n.rochefort@ed.ac.uk

Abstract

Mammals have evolved sex-specific adaptations to reduce energy usage in times of food scarcity. These adaptations are well described for peripheral tissue, though much less is known about how the energy-expensive brain adapts to food restriction, and how such adaptations differ across the sexes. Here, we examined how food restriction impacts energy usage and function in the primary visual cortex (V1) of adult male and female mice. Molecular analysis and RNA sequencing in V1 revealed that in males, but not in females, food restriction significantly modulated canonical, energy-regulating pathways, including pathways associated with AMP-activated protein kinase (AMPK), peroxisome proliferator-activated receptor alpha (PPARα), mammalian target of rapamycin (mTOR), and oxidative phosphorylation. Moreover, we found that in contrast to males, food restriction in females did not significantly affect V1 ATP usage or visual coding precision (assessed by orientation selectivity). Decreased serum leptin is known to be necessary for triggering energy-saving changes in V1 during food restriction. Consistent with this, we found significantly decreased serum leptin in food-restricted males but no significant change in food-restricted females. Collectively, our findings demonstrate that cortical function and energy usage in female mice are more resilient to food restriction than in males. The neocortex, therefore, contributes to sex-specific, energy-saving adaptations in response to metabolic challenge.

Introduction

Mammals reduce their energy usage in times of food scarcity. These adaptations have been well documented for peripheral tissues and are sex-specific. For example, females, as compared to males, readily lose muscle and bone mass to reduce peripheral energy expenditure during food restriction, but lose less fat mass and overall bodyweight[1–6]. Moreover, females are more likely to suppress energy-costly, reproductive functions during food restriction than males, evidenced by substantive reductions in uterine and ovarian mass, as well as a cessation of reproductive function and behaviour[7–9]. Such sex-specific differences are thought to reflect the differential importance of different organs to sex-specific survival[2].

In contrast to peripheral tissue, whether and how the brain adapts its function and energy use in a sex-specific manner during food scarcity remains largely unknown. The brain requires substantial amounts of energy to process and encode information[10–12]. Indeed, the human brain, which comprises 2% of our body's mass, consumes 20% of our caloric intake, over half of which is used by the cerebral cortex[12]. Previously, we demonstrated that food restriction in male mice reduced energy usage in the primary visual cortex (V1) during visual processing, which was associated with a loss of orientation selectivity and visual coding precision[13]. These changes required a decrease in levels of serum leptin, a hormone secreted by adipocytes in proportion to fat mass[14]. Thus, in males the cortex, like peripheral tissue, has the capacity to reduce its energy usage and function in times of food scarcity.

By contrast, it remains unclear to what extent the brain similarly contributes to energy-saving adaptations during food scarcity in mammalian females. Understanding how food restriction impacts cortical function in males and females is not only of fundamental importance for understanding the sex-specific impact of diet on brain function, but is also critical for studies of cortical function, in which food restriction is used to behaviourally motivate animals[15–17].

Here, we examined how food restriction leading to a 15% loss in body weight over 2-3 weeks impacts energy usage and visual coding in the primary visual cortex (V1) in adult male and female mice. We found that leptin levels, which regulate energy-saving changes in[13], were maintained in females during food restriction, despite being decreased by approximately threefold in males. Consistent with these results, and using a range of experimental techniques, we failed to find significant energy-saving changes in V1 during food restriction in female mice, in contrast to male mice. Specifically, molecular analysis and RNA sequencing of V1 revealed that food-restriction significantly modified canonical energy-regulating cellular pathways in males, but not in females, including pathways associated with AMP-activated protein kinase (AMPK), peroxisome proliferator-activated receptor alpha (PPARα), and mammalian target of rapamycin (mTOR) signalling, as well as

oxidative phosphorylation. Moreover, using *in vivo* ATP and calcium imaging, we found that food restriction significantly reduced V1 ATP use and orientation selectivity in males, but not in females.

Collectively, our study demonstrates that in times of food restriction, visual cortical function and energy usage are largely maintained in female mice, while they are reduced in males. The neocortex, therefore, contributes to sex-specific, energy-saving adaptations in response to metabolic stress. Our research highlights the importance of taking into account sex differences when studying the impact of dietary manipulations on brain function.

Results

We first examined sex-specific differences in how the neocortex adapts to food restriction in mice. Mice, 7-9 weeks of age, either had *ad libwitum* (CTR) access to food or were food restricted (FR) to 85% of their free feeding bodyweight, for 2-3 weeks (Figure 1A). Prior to any of our recordings, tissue collection, and analysis, all animals were given *ad libitum* access to food until sated. This enabled us to examine the long-term impact of caloric restriction on neocortical function, as opposed to the short-term impacts of hunger[18,19].

Sex-specific impact of food restriction on weight loss and fat mass-regulated hormone leptin

Prior to food restriction, we found that both males and females consumed the same *ad libitum* daily food intake, despite females weighing approximately 80% of age-matched males (weight: male vs. female; 29.42±0.20g vs 24.23±0.54g; t-test: $p < 0.001$; n = 8 male mice and 7 female mice). Critically, we found that to achieve a similar magnitude (15%) and rate of weight loss in both sexes we had to impose a 40% greater restriction of daily food intake in females (average of 39% of *ad libitum* intake; n = 7 female mice) compared to males (27% of *ad libitum* intake; n = 8 male mice) (Figure 1B,C). This is consistent with previous studies demonstrating that female mice are more resistant to weight loss than male[1–6]. Moreover, for similar bodyweight loss (15%) maintained over 2-3 weeks, serum leptin levels, which reflect fat mass, were markedly and significantly decreased (-72%) in males (t-test: $p < 0.001$; n = 17 control male mice and n = 19 food-restricted male mice), but only modestly and non-significantly decreased (-28%) in females (t-test: $p = 0.32$; n = 23 control female mice and n = 11 food-restricted female mice) (Figure 1D). This is in keeping with previous findings that female mice are more resistant to fat loss than males[1–6] and that weight loss arises from other tissues including those associated with reproductive functions (ovarian and uterine mass)[7–9].

Cellular energy-regulating pathways in cortex are significantly impacted by food restriction in males but not in females

Decreased leptin levels are necessary for triggering energy-saving changes in the mouse visual cortex during food restriction[13]. We therefore asked whether the absence of significant change in serum leptin in food-restricted females was associated with any change in V1 energy usage. We first assessed this at the molecular level by examining AMPK phosphorylation state. AMPK is a canonical cellular energy sensor activated by metabolic stress - such as food restriction, in part via decreased leptin signalling - through phosphorylation of threonine 172 (Thr^{172})[20–22]. Its activation results in reduced ATP expenditure, for example, through the inhibition of mammalian target of rapamycin (mTOR) signalling[20,23], and regulation of mitochondrial oxidative phosphorylation[24,25]. In V1, we found that AMPK Thr^{172} phosphorylation was markedly and significantly elevated (2.9 fold) with food restriction in males ($p < 0.05$; n = 11 control male mice and n = 15 food-restricted male mice), consistent with ATP savings, but only modestly increased (1.4 fold) in females; this increase was not statistically significant ($p = 0.11$; n = 11 control female mice and n = 6 food-restricted female mice) (Figure 1E). We also examined the activity of peroxisome proliferator-activated receptor alpha (PPARα), which is downstream of leptin signalling and is known to regulate fatty acid metabolism and energy homeostasis[22,26]. As with AMPK, we found that PPARα was significantly regulated by food restriction selectively in males, but not in females (Figure 1E)[27,28].

To further investigate how energy-regulating cellular pathways are impacted by food restriction, we performed RNA sequencing on tissue dissected from V1 (Figure 2A; n = 4 control male, n = 4 food-restricted male, n = 4 control female, and n = 4 food-restricted female mice). Differential gene expression analysis using DESeq2 revealed that food restriction significantly altered the expression of 657 and 585 targets in males and females, respectively (at a threshold of p-adj ≤ 0.1; only 125 of these were common to both sexes (Figure 2B). To assess the functional relevance of the transcriptomic changes induced by food restriction, we performed Gene Set Enrichment Analysis (GSEA) to identify pathways enriched in the differentially expressed populations. We found that food restriction resulted in a significant alteration of 34 and 14 gene sets (at p-adj ≤ 0.05) in males and females respectively; 13 of these were common to both sexes (Figure 2C; Table 1; Table 2). In male mice, we specifically found that food restriction significantly regulated gene sets associated with canonical energy-regulating pathways (Figure 2), including those associated with oxidative phosphorylation and mTOR signalling (mTORC1 signalling and PI3K/AKT/mTOR signalling), as well as fatty acid metabolism; these pathways are known to regulated by leptin and AMPK signaling[20,27–29] (Figure 2D). Notably, these pathways were not significantly regulated by food-restriction in females. In addition to these findings, we found that gene sets associated to estrogen-regulating pathways

were significantly regulated in food-restricted males and not in females (Figure 2C). This is consistent with previous findings showing that estrogen, like leptin, suppresses food intake and promotes energy expenditure[30]. Finally, consistent with past studies in cortex, we found that food restriction in males altered gene expression associated with inflammation and reactive oxidative species (Figure 2D)[31,32].

Collectively these findings reveal that food restriction strongly affects energy-regulating cellular pathways in the cortex of male, as opposed to female, mice.

ATP usage in V1 is significantly decreased under food restriction in males but not in females

We next examined energy usage in visual cortex during visual processing using two photon ATP imaging in V1 of awake, head-fixed Thy1-ATeam1.03^{YEMK} mice, which express a FRET-based ATP sensor[33,34] (Figure 3A). In the presence of ATP synthesis inhibitors, focally applied over the visual cortex, ATP usage can be seen as a decay of the FRET signal during visual stimulation with natural stimuli[13] (Figure 3A). Data obtained in females were compared to our previously published datasets obtained under similar conditions in male mice[13]. As previously shown[13], food restriction robustly decreased the rate of cortical ATP usage in males (24% decrease) (t-test: $p < 0.01$; n = 11 control male mice and n = 10 food-restricted male mice); a more modest trend was observed in females (12% decrease), which was not significant compared to controls (t-test: $p = 0.18$; n = 12 control female mice and n = 8 food-restricted female mice) (Figure 3B-C). These findings demonstrate that food-restriction significantly impacts V1 energy usage in males but not in females.

Orientation selectivity in V1 is significantly reduced under food restriction in males but not in females

We next examined how food restriction impacts visual cortical function. In male mice, reductions in energy usage in V1 during food restriction are associated with a decreased visual coding precision as evidenced by a reduction of orientation selectivity[13]. Given the non-significant impact of food-restriction on energy usage in female mice, we reasoned that orientation selectivity would also be less impacted. We analysed two-photon calcium imaging data of V1 GCaMP6s-labeled layer 2/3 neurons in female mice viewing drifting gratings (Figure 3D-F; n = 7 control male, n = 8 food-restricted male, n = 7 control female, and n = 9 food-restricted female mice). Data obtained in females were compared to our previously published datasets obtained under similar conditions in male mice[13]. Consistent with our hypothesis, in contrast to males in which orientation selectivity was significantly reduced by 27% ($p<0.001$), orientation selectivity was modestly and not significantly reduced by food-restriction in females (13%; $p=0.08$) (Figure 3E-F).

Altogether, our results show that energy usage and coding precision in the visual cortex are largely maintained in female mice under food restriction while they are robustly reduced in males.

Bayes factor analysis reveals statistically robust impact of metabolic stress on V1 energy use and visual coding in males, but not females

We used Bayes factor hypothesis testing to better assess the statistical impact of food restriction on visual cortical function and energy use in male and female mice (Supplemental Figure 1). Bayes factor analysis uses a Bayesian framework to quantify how much more likely the data is under the alternative hypothesis (*i.e.* there is an effect of food restriction) versus the null hypothesis (*i.e.* there is no effect of food restriction), quantified by the Bayes factor (BF_{10})[35,36]. A $BF_{10} > 3$, for example, means that the data is >3 times more likely under the alternative hypothesis than the null hypothesis. Critically, the BF_{10} allows for a more informative comparison of the effects of food restriction between sexes, as opposed to comparing p-values, which can be misleading[35,36]. Across the parameters of energy use and visual coding that we tested (Figures 1-3), BF_{10} for males was consistently several-fold greater than that for females. Thus, visual cortical function and energy use was more robustly modulated by food restriction in males than in females.

Our findings however cannot rule out a potential, smaller impact of food restriction on cortical function and energy use in females, below the threshold for statistical detection in this study. The Bayes factor analysis helps to differentiate the absence of evidence from the evidence of absence. In particular, moderate evidence in support for the absence of an effect requires a $BF_{10} < 0.33$ (*i.e.* the data is 3 times more likely under the null hypothesis than the alternative hypothesis)[35,36]. For females, we found only 3 out of the 10 parameters had $BF_{10} < 0.33$ (Supplemental Figure 1), suggesting that food restriction may have a modest impact on V1 energy use or function, but below the limits of statistical detection in our study. Altogether, our results show that energy usage and coding precision in the visual cortex are largely maintained in female mice under food restriction while they are robustly reduced in males.

Discussion

Here, we find that in female mice, energy usage and visual coding in V1 is largely unchanged under food restriction. Using molecular analysis and RNA sequencing, we found that energy-regulating pathways were not significantly changed with food restriction in females, in contrast to males; these included pathways associated with AMPK, mTOR, and PPARα signalling, as well as oxidative phosphorylation. Consistent with this, we found that food restriction in females did not impact visual cortical ATP usage nor orientation selectivity, both of which were reduced by food restriction in males.

Our findings suggest that the contribution of neocortex to energy-saving adaptations during food restriction is sex-selective and more pronounced in males; females may rely on other energy-saving strategies, such as reducing reproductive function, to cope with food restriction.

Limitations of the study

Our study focused on the effects of a moderate food restriction protocol over 2-3 weeks on neocortical function and energy use. This protocol is widely used in metabolic studies investigating the impact of caloric restriction on peripheral physiology, as well as in neuroscience studies to motivate rodents to perform specific behaviors[6,15–17]. However, it remains unclear to what extent our findings generalize to other protocols of food restriction. Indeed, the duration, magnitude, and pattern of food restriction, as well as macronutrient composition are known to impact the physiological responses to dietary manipulations[22,37–39]. Moreover, whilst we focussed our study on the adult visual cortex, it remains unclear if the brain shows similar sex-specific energy-saving adaptations in other cortical areas, and how such adaptations change with age[6,40].

A key strength of our study is that we consistently found, across a number of experimental methods, that changes in cortical function and energy use were significant in males, but not in females. However, a critical limitation of our study is that we did not have the statistical power to directly compare the effect size of food restriction between the sexes (e.g. ANOVA interaction effects); to do so would require a substantial increase in experimental group sizes by several fold. We addressed this limitation, in part, using Bayes factor analysis, which revealed that the impact of food restriction in males was indeed more robust than in females. This analysis also revealed that our study did not have sufficiently strong evidence to definitively rule out a smaller effect of food restriction in females, which may not have been statistically detectable.

Role of leptin and sex hormones in food restriction impact on cortical activity

Consistent with past studies, we found that food-restricted female mice resisted weight loss, and therefore required a greater restriction of food to achieve similar weight loss (relative to baseline) as males. In addition, for the same relative weight loss as males, females exhibited minimal reductions in serum leptin levels (secreted by adipocytes), consistent with past studies showing that females resist fat loss during food restriction[1–3,5,6]. Similar effects have been observed across several mammalian species, including humans, and is thought to reflect the differential importance of fat stores for reproductive success in males and females[1–5]. Notably, we previously demonstrated that reductions in leptin levels during food restriction are necessary for driving energy-saving changes in visual cortical coding in male mice; leptin therefore acts as a critical signal linking the neocortex to fat stores[13]. That leptin levels are not significantly affected by food restriction in females may explain the minimal impact food restriction has on cortical energy usage and coding precision in female mice.

In addition to leptin, sex hormones likely contribute to sex-specific adaptations to food restriction[41]. As with leptin, estrogen suppresses food intake and promotes energy expenditure[30], in part by augmenting leptin signalling by increasing leptin-induced phosphorylation of STAT3[42]. Moreover, estrogen can enhance ATP production by sensitizing insulin signalling, enhancing glycolysis and oxidative phosphorylation, and along with progesterone, upregulating mitochondrial gene expression and function[30,43,44]. Interestingly, in our study, RNA sequencing revealed that estrogen signalling pathways were significantly regulated in male visual cortex with food-restriction, and were unchanged in females. Estrogen may thus have overlapping effects with those induced by food restriction, thereby diminishing further responses to food restriction in females[6]. Notably, it was recently shown that sex differences in calorie-restriction's metabolic effects that are observed in young adult mice, are largely absent in older mice, when females' estrogen levels have declined[6]. Further studies will be needed to explore whether the resilience of cortical function found in this study in young cycling adult females is also observed in non-cycling mice with reduced oestrogen levels, such as in aged mice.

Sex-specific regulation of cellular energy-regulating pathways

AMPK and mTOR signalling pathways are canonical regulators of cellular energy usage[20,23]. We found these pathways, along with cortical ATP usage, to be significantly modulated by food-restriction in male, but not female mice. AMPK is activated during metabolic stress, and saves energy by regulating oxidative phosphorylation[24,25], and inhibiting cellular pathways associated with energy usage, such as mTOR signalling[20]. mTOR signalling, by upregulating protein synthesis, increases ATP use by promoting neuronal excitability, neurite outgrowth, ion channel expression, and synaptic plasticity[23]. mTOR signalling is therefore ideally situated to regulate how much ATP is used in neuronal function; its inhibition may underlie ATP savings and the associated loss of coding precision with food-restriction in male mice. Notably, previous studies have found sex- and tissue- dependent regulation of AMPK and mTOR signalling, including in response to food restriction[41]. For example, in skeletal muscle, mTOR signalling is enhanced by fasting selectively in male, but not female mice[41,45]. Moreover, metabolic challenge by endurance training induces greater AMPK activity in cardiac tissue in male, as opposed to female mice[46]. Our study extends the sex-specific regulation of these energy-regulating pathways to the neocortex.

Importance of biological sex on the impact of food restriction on cortical function.

Food restriction protocols are widely used to motivate animals in behavioural studies examining cortical function[15–17]. Our findings suggest that these protocols are likely to have greater impacts on

basal neocortical function in males, as compared to females. Consistent with this, a recent study has found that food restriction in juvenile mice strongly impacts cognitive flexibility in learning and decision-making in adulthood, specifically for males but not females[47,48]. Such sex-specific impacts of food restriction on neocortical function are important to take into consideration in the design and interpretation of such studies.

Diet is known to have a considerable impact on neurological diseases, including epilepsy, Alzheimer's disease, and other neurodegenerative diseases[49,50]. Whilst calorie restricted diets have proven to be of benefit in this regard, the sex-dependency of such interventions have not been thoroughly investigated, though on the basis of our findings it is conceivable that males and females may respond differently to dietary interventions. The inclusion of both males and females in biomedical research, and the study of sex differences, is therefore of considerable importance for ensuring efficacious treatments are developed for both sexes.

In conclusion, we find that visual cortical coding and energy usage in females are resistant to food restriction, in contrast to males. Our findings establish that sex-specific adaptations in energy usage, previously described in peripheral tissue under metabolic challenge, extends to the neocortex.

Acknowledgments

We thank the GENIE Program and the Janelia Research Campus (V. Jayaraman, R. Kerr, D. Kim, L. Looger, and K. Svoboda) for making GCaMP6 available. We thank J. Hirrlinger (Carl Ludwig Institute of Physiology, University of Leipzig, Germany) for providing the ATeam1.03^{YEMK} mouse line. We thank Sang Seo and Aditi Singh for assistance and guidance in RNA sequencing and analysis. We thank Will Cawthorn for discussions on the manuscript. This work was funded by the BBSRC (Responsive Mode Research Grant (BB/T007907/1 to N.R. and Z.P.), the Royal Commission for the Exhibition of 1851 (research fellowship to Z.P.), the MRC (Career Development Fellowship to Z.P.), the Wellcome Trust and the Royal Society (Sir Henry Dale fellowship to N.R.), the Shirley Foundation, the Patrick Wild Centre, the RS MacDonald Charitable Trust Seedcorn Grants (to N.R. and Z.P.), the Simons Initiative for the Developing Brain (to N.R. and D.K.) and the Wellcome Trust-University of Edinburgh Institutional Strategic Support Fund (ISSF3) (to N.R.). This project has received funding from the European Research Council (ERC) under the European Union's Horizon 2020 research and innovation programme (grant agreement No. 866386).

Author contributions

Z.P. and N.R. designed the experiments. Z.P. performed and analysed calcium imaging experiments and ELISAs. D.K. performed and analysed calcium and ATP imaging experiments. Z.P. and M.R. and

302 E.O. processed tissue for RNA sequencing and analyzed data. P.M. performed and analyzed ELISAs.
303 N.R. supervised the project. Z.P. and N.R. wrote the manuscript with input from all authors.
304

305 Declaration of Interests

306 The authors declare no competing interests.
307

308 Inclusion and Diversity

309 One or more of the authors of this paper self-identifies as an underrepresented ethnic minority in
310 science. One or more of the authors of this paper self-identifies as a member of the LGBTQ+
311 community. While citing references scientifically relevant for this work, we also actively worked to
312 promote gender balance in our reference list.
313

314 Figure Legends

315 **Figure 1. Sex-specific impact of food restriction on weight loss and serum leptin.** (A) Animal weight
316 across time. (B) Daily food intake (two-way ANOVA: CTR male vs. CTR female; $p = 0.99$; FR male vs. FR
317 female; $p = 0.07$; n = 8 CTR males, 8 FR males, 7 CTR females, and 7 FR females). Percent reduction of
318 food intake for food restriction is shown in red for each sex. (C) Animal weight (two-way ANOVA: n =
319 17 CTR males and 19 FR males; 22 CTR females and 11 FR females). (D) Serum leptin levels (two-way
320 ANOVA: CTR females vs FR females; $p=0.32$; n = 17 CTR males and 19 FR males; 22 CTR females and
321 11 FR females). (E) Left. AMPK Thr172 phosphorylation, normalized by total AMPK, in primary visual
322 cortex (V1) tissue (two-way ANOVA: CTR female vs. FR female; $p = 0.11$; n = 11 CTR males, 15 FR males,
323 11 CTR females, and 6 FR females). Right. PPARα activity in V1 tissue, as assessed by levels of DNA
324 binding, normalized to protein level (two-way ANOVA: CTR female vs. FR female; $p = 0.99$; n = 5 CTR
325 males, 11 FR males, n = 9 CTR females, and 9 FR females). $^*p < 0.05$; n.s. = not significant. Error bars
326 are S.E.M.
327

328 **Figure 2. Cellular energy-regulating pathways are more robustly impacted by food restriction in**
329 **males than in females.** (A) Schema of RNA sequencing of V1 tissue. (B) Volcano plot of fold change
330 expression with food restriction vs. significance for all analyzed genes; broken horizontal line denotes
331 adjusted $p \leq 0.1$ significance level, below which non-significantly regulated expressed genes are
332 marked by grey. Inset: Venn diagram showing the number of significantly differentially expressed
333 genes with food restriction in males and females. (C) Gene Set Enrichment Analysis using Hallmark
334 Gene Sets, depicted using a volcano plot of Enrichment Score vs. significance for males (left) and

335 females (right); broken horizontal lines denotes adjusted $p \leq 0.05$ significance level. Inset: Venn
336 diagram showing the number of significantly regulated gene sets with food restriction in males and
337 females. (D) Complete list of significantly enriched gene sets by food-restriction in males and females
338 for analysis in C. Gene sets of interest are denoted by a box. All data from 4 CTR males, 4 FR males, 4
339 CTR females, and 4 FR females.
340
341 **Figure 3. ATP use and orientation selectivity in V1 is more robustly decreased by food restriction in**
342 **males.** (A) Schemata of ATP imaging experiment. Top: example field of view of V1 layer 2/3 neurons
343 in the ATeam1.03^{YEMK} transgenic mouse (scale bar: 10 µm). Bottom: ATP synthesis inhibitors were used
344 to isolate ATP usage, recorded as a decrease in FRET signal during presentation of natural, outdoor
345 scenes. (B) Normalized ATeam1.03^{YEMK} FRET signal in males and during presentation of natural,
346 outdoor scenes. ATP synthesis inhibitors (arrow) were added to isolate ATP usage. Inset: Time to 50%
347 decay of the ATeam1.03^{YEMK} FRET signal (two-way ANOVA; n = 11 CTR males and 10 FR males). (C) As
348 in (B) but for females (inset: two-way ANOVA; p = 0.18; n = 12 CTR females and n = 8 FR females). (D)
349 Top: Schema of two-photon imaging and sample field of view of V1 layer 2/3 neurons expressing
350 GCaMP6s (scale bar: 10 µm). Bottom: Sample fluorescent signals (grey) from a selected neuron (black
351 circle) in response to 6 drifting gratings of varying orientations. Trial averages are in black. Horizontal
352 bar denotes 2s grating presentation. (E) Mean orientation tuning normalized to the response to the
353 preferred orientation for CTR and FR males (data from [13]). Note that -90° and +90° conditions
354 correspond to the same visual stimulus. Inset: Orientation selectivity index (OSI; two-way ANOVA; n =
355 8 CTR and 8 FR males). (F) As in (E) but for females (Inset: two-way ANOVA; p = 0.08; n = 7 CTR females
356 and 9 FR females). **p < 0.01; ***p < 0.001; n.s. = not significant. Error bars are S.E.M. Data from male
357 mice are from a previously published dataset obtained under similar conditions[13].
358
359 **Supplemental Figure 1. Bayes factor analysis reveals statistically robust impact of metabolic stress**
360 **on V1 energy use and visual coding in males, but not in females.** Bayes factor (BF_{10}) along with
361 quantified effect size and 95% confidence intervals (CI) are shown for males (green) and females
362 (purple). Across parameters, BF_{10} and effect sizes are greater for males than females, meaning that
363 food restriction induces a more robust effect on visual cortical function and energy use in males than
364 females.
365
366
367 ## STAR METHODS
368

RESOURCE AVAILABILITY

Lead contact

Further information and requests for resources and materials should be directed to and will be fulfilled by the lead contact Nathalie L. Rochefort (n.rochefort@ed.ac.uk).

Materials availability

This study did not generate new unique reagents.

Data and code availability

1. GEO accession number for RNA-seq datasets: GSE233435
2. Processed data will be made available at https://datashare.ed.ac.uk/handle/10283/3871. Requests for raw data should be made to and will be fulfilled by the lead contact (n.rochefort@ed.ac.uk).
3. MATLAB scripts to analyse data have been previously published[13] and are available at https://zenodo.org/record/5561795#.YmJ3AtrMJPY and https://github.com/rochefort-lab/Padamsey-et-al-Neuron-2022.
4. Any additional information required to reanalyze the data reported in this paper is available from the lead contact upon request.

EXPERIMENTAL MODEL AND SUBJECT DETAILS

Experiments were approved by the University of Edinburgh's Animal Welfare and Ethical Review Board (AWERB) and carried out under Home Office (UK) approved project and personal licenses. All experiments conformed to the UK Animals (Scientific Procedures) Act 1986 and the European Directive 86/609/EEC and 2010/63/EU on the protection of animals used for experimental purposes.

This study used male and female C57BL/6J mice (RRID:IMSR_JAX:000664; Jackson Laboratory) and male B6-Tg (Thy1.2-ATeam1.03^{YEMK})^{AJhi} transgenic mice, that were bred on a C57BL/6J background (RRID:MGI:5882597; https://scicrunch.org/resources). Animals were group housed (2-5 animals/cage) and maintained on a reverse light/dark (12h/12h) cycle in a room kept at 21±2°C and 55±10% humidity.

401 For data associated with *in vivo* recordings (Figure 3), data obtained in female mice were compared
402 to our previously published datasets obtained under similar conditions in male mice[13]
403
404 **METHOD DETAILS**
405
406 **Food restriction**
407 Mice (7-9 weeks of age) either had *ad libitum* access to food (RM1 expanded pellets; DBM Scotland
408 UK) or were food restricted for 2-3 weeks to 85% of their baseline bodyweight prior to
409 experimentation as previously described[13]. Briefly, for food restriction, one ration of food was given
410 4-8 hours prior to the end of the dark cycle, with the amount of food progressively reduced to achieve
411 target weight. 1-2 hour prior to experimentation, all animals had *ad libitum* access to food until sated.
412
413 **AAV injection and cranial window**
414 For calcium imaging experiments, C57BL6 were anesthetized using isoflurane, and given pre-operative
415 analgesia (vetergesic: 0.1 mg/kg; carprieve: 5 mg/kg; rapidexon: 2 mg/kg) along with warm Ringer's
416 solution (25ml/kg) subcutaneously; vetergesic jelly was additionally given orally post-operatively 24
417 hours later. Opaque eye cream was applied to the eyes (Bepanthen, Bayer, Germany). A craniotomy
418 (2x2 mm) was applied over left V1 (centre at 2.5 mm mediolateral and 0.5 mm anterior to lambda).
419 Flexed GCaMP6S (AAV1.Syn.Flex.GCaMP6s.WPRE.SV40; Addgene; RRID:Addgene_105558-AAV1)
420 diluted 1:10 in saline, along with CaMKII-dependent Cre-recombinase (AAV1.CamKII 0.4.Cre.SV40;
421 Addgene; RRID:Addgene_105558-AAV1) diluted 1:100 saline was injected at the centre of the
422 craniotomy via a sharp glass pipette. Injections were targeted to layer 2/3, with 100 nL of virus solution
423 injected (2.5nL/30s) at each of 3 depths (150, 250 and 350 µm) via a sharp glass pipette using a
424 Nanoject III (Drummond Scientific). A glass window was then used to seal the craniotomy, and
425 superglued in place. The window was made of 1 or 2 glass coverslips (Menzel-Glaser # 0), in the latter
426 case the 2 cover slips were glued together with optically-clear, UV-cured glue (Norland Optical
427 Adhesive no. 60); the inner window was 2.0 mm x 2.0 mm, the outer window was 2.5 mm x 2.5 mm.
428 A metal headplate was then fixed to the skull with super glue and dental cement (Paladur, Heraeus
429 Kuzler). It took 3-6 weeks for viral expression prior to experimentation.
430
431 For ATP imaging experiments, we used ATeam1.03^{YEMK} mice (RRID:MGI:5882597;
432 https://scicrunch.org/resources) that express a FRET-based sensor under the Thy1 promoter[33]. One
433 the day of experimentation, animals were anesthetized with isoflurane and given pre-operative
434 analgesia (Carprieve: 5 mg/kg) and 25 mL/kg of warm Ringer's solution subcutaneously. A headplate

435 was first fixed to the skull with superglue and dental cement, after which a small craniotomy (~0.5 x
436 ~0.5 mm) was made over left V1 (centre at 2.5 mm mediolateral and 0.5 mm anterior to lambda),
437 which was covered with agarose (1-2%) and silicone. Following recovery from anaesthesia (30-60
438 minutes) the animal was head-fixed; the agarose and silicone were removed and replaced with HEPES-
439 buffered ACSF (in mM: 124 NaCl, 20 Glucose, 10 HEPES, 2.5 KCl, 1.2 NaH_2PO_4, 2 $CaCl_2$, and 1 $CaCl_2$; pH
440 7.2-7.4).
441
442 **Habituation and Head-fixation**
443 During imaging, mice were placed in a cardboard tube and head fixed. Prior to the imaging day, mice
444 were handled daily for 2-3 weeks prior, and exposed to cardboard tubes, similar to the one on the
445 experimental rig. They were also habituated to the rig via once daily, 10-15 minute sessions for 2 days
446 prior to recording. For ATP imaging, mice were habituated to the experimental setup without head
447 fixation (10-15 min session/day for 1-2 days).
448
449 ***In vivo* two-photon imaging**
450 ATP and calcium imaging were using a two-photon resonant scanning microscope, as previously
451 described[51–53], which was equipped with a Ti:Sapphire laser (Charmeleon Vision-S, Coherent, CA) and
452 GaAsP photomultiplier tubes (Scientifica), and controlled with LabView (v8.2; National Instruments,
453 UK). Time-series xy images were acquired at 40Hz using a 25x water-immersion objective (Nikon;
454 CF175 Apo 25XC W; 1.1 NA) at depths between 160 and 280 µm below the pia. For GCaMP6s imaging,
455 excitation was tuned to 920nm. For ATP imaging (CFP/YFP FRET sensor), the laser was tuned to 850
456 nm for CFP excitation. CFP and YFP fluorescence were recorded simultaneously using a 515nm long-
457 pass dichroic mirror with the following emission filters: 485/70nm for CFP and 535/45nm for YFP
458 (mirror and filter set: T515lpxr C156624; Scientifica). Imaging data was acquired during the
459 presentation of visual stimuli, with at least 10 replicate trials for each visual stimulus. For ATP imaging,
460 three trials were taken at baseline, then ACSF containing ATP synthesis inhibitors (1 mM oligomycin
461 and 20 mM sodium iodoacetate) was applied over the open craniotomy isolate ATP usage. Thirty trials
462 were successively performed immediately after drug application. For in vivo recordings, data obtained
463 in females were compared to our previously published datasets obtained under similar conditions in
464 male mice[13].
465
466 **Visual Stimuli**
467 MATLAB (Mathworks; RRID:SCR_001622; Psychophysics Toolbox; RRID:SCR_002881) was used to
468 generate drifting grating stimuli. These were displayed on an LCD monitor (51 x 29 cm; Dell) placed 20

469 cm from the right eye, contralateral to the hemisphere with the cranial window. For food restriction
470 experiments, on a given trial, 12 full-field drifting gratings (drift angle: 0, 30, 60, 90, 120, 180, 210,
471 240, 270, 300, 330°; temporal frequency = 1 Hz), 2 s in duration, were presented in random order,
472 interspersed with grey screens (4 s duration). Gratings within a trial were randomly assigned one
473 common spatial frequency (0.02, 0.04, 0.16, or 0.32 cpd). For natural stimuli, a 60s movie was
474 presented of an outdoor movie of movement through a field and vegetation.

475 **Serum leptin measurements**

476 Serum leptin levels were analyzed using ELISA kits (Mouse Leptin Quantikine Elisa Kit, R&D Systems,
477 USA) according to manufacturer's instruction. For serum collection, trunk blood was collected from
478 mice that were briefly anesthetized (isoflurane) prior to decapitation. Blood was allowed to clot at
479 room temperature for 1-2 hours and then centrifuged for 20 minutes at 2000 x g. The serum was
480 drawn off and stored at -80°C until used.

481

482 **AMPK and PPARα measurements**

483 Levels of total AMPK, phosphorylated AMPK (Thr172), and nuclear PPARα in V1 were measured using
484 ELISA kits according to manufacturer's instructions (total AMPK: ab181422, Abcam, UK;
485 phosphorylated AMPK: KHO0651, ThermoFisher, UK; PPARα: ab133107, Abcam, UK). For tissue
486 collection, mice were briefly anesthetized (isoflurane) and decapitated. The visual cortex was
487 dissected out, snap frozen using dry ice, and stored at -80°C until used.

488

489 **RNA sequencing**

490 Bulk RNA sequencing was performed on V1. V1 tissue was collected and snap frozen from mice that
491 were briefly anesthetized (isoflurane) and decapitated. Tissue was homogenized using a bead mill
492 (Bead Mill 24, Fisher Scientific) and RNA was isolated using an RNeasy kit (Qiagen) according to
493 manufacturer's instructions. RNA integrity was confirmed (RIN > 7) and mRNA was sequenced at the
494 Oxford Genomics Centre using Illumina NovaSeq 6000.

495 **QUANTIFICATION AND STATISTICAL ANALYSIS**

496 **Ca^{2+} Imaging Analysis**

497 Image analysis for calcium imaging was performed as previously described[45,47,49]. For motion correct,
498 a discrete Fourier 2D-based image alignment was used (SIMA 1.3.2)[53]. Regions of interest (ROI) were
499 manually drawn around imaged neuronal soma using ImageJ software (NIH public domain;
500 RRID:SCR_002285). Pixel fluorescence was then averaged within each ROI to generate a time series.
501 For each ROI, baseline fluorescence (F_0) was calculated by taking the 5th percentile of the smoothed

time series (1 Hz lowpass, zero-phase, 60th-order FIR filter). ΔF/F was then calculated as ($F-F_0/F_0$). FISSA was used to decontaminate the neuropil[55]. Subsequent analyses were performed using custom scripts in MATLAB (MathWorks)[13].

Drifting grating analysis

The visual response to drifting gratings was defined as the highest mean ΔF/F, averaged within a 2s window, that occurred within a 4 s window (comprising the 2s grating presentation plus the 2 s of the grey screen presentation which immediately followed the grating presentation). The visual response was subtracted by baseline ΔF/F, defined as the mean value within a 1 s window prior to the visual response.

Responses to gratings of the same angle, but different drift directions were averaged together. Given that multiple spatial frequencies were used, only the spatial frequency with the largest response, meaned across all orientations, was selected for each neuron for subsequent analyses. A neuron's preferred orientation was that which evoked the largest mean response.

Grating responsive neurons were defined as those for which grating responses were better fit with a double Gaussian curve (direction responses) than with a flat line at zero (null model), which was determined using Bayesian Information Criterion (BIC)[13]. The double Gaussian curve was defined as:

$$R(\theta) = C + R_p e^{\frac{-ang_{dir}(\theta-\theta_{pref})^2}{2\sigma^2}} + R_n e^{\frac{-ang_{dir}(\theta-\theta_{pref})^2}{2\sigma^2}}$$

Where R (θ) is the response at a given direction angle θ, C is an offset, R_p is the response to the preferred direction after subtracting the offset, θ_{pref} is the angle of the preferred direction, R_n is the response to the null direction after subtracting the offset, and $ang_{dir}(x) = \min(x, x-360, x+360)$, which constrains angular differences to 0-180°, and σ is the standard deviation of the curve.

BIC was given by:

$$BIC = nln(\overline{\sigma^2}) + kln(n)$$

Where n is the number of responses, $\overline{\sigma^2}$ is the mean residual sum of squares of the model, and k is the number of free parameters used by the model, which was zero in the case of the null model. A

535 neuron was considered significantly grating-responsive if the BIC_{null} - $BIC_{Gaussian} \geq 10$, which provides
536 strong evidence against the null model[54].
537
538 **Orientation selectivity**
539 The orientation selective index (OSI) of grating-responsive neurons was calculated as 1 – circular
540 variance based on the mean response of the neuron to each; values less than zero were set to zero.
541 OSI was given by:
542
543 $$OSI = abs\left(\frac{\sum_k R(\theta_k)e^{2i\theta_k}}{\sum_k R(\theta_k)}\right)$$
544
545 Where R (θ_k) is the response to the k_{th} angle θ. The average OSI for an animal was taken as the median
546 OSI value calculated across neurons.
547
548 **ATP measurements**
549 For ATeam1.03^{YEMK} imaging, CFP and YFP fluorescence was averaged across ROIs drawn around visible
550 soma in the field of view, after background subtraction. FRET was calculated as a ratio of YFP/CFP
551 fluorescence, and decayed as a function of time with visual stimulation in the presence of ATP
552 synthesis inhibitors. The FRET signal was bound between 0 and 1 by first subtracting the mean FRET
553 signal during the last 3 imaging trials (the FRET signal plateaued at this point), and then dividing by the
554 mean FRET signal at baseline. The FRET decay half time was defined as the time required for the FRET
555 to decay to 50% of its baseline value.
556
557 **Differential gene expression analysis**
558 RNA sequencing reads were mapped, using STAR 2.4.oi, to the *Mus musculus* primary assembly
559 (Ensembl v80)[55]. FeatureCounts 1.4.6-p2 was used to count reads uniquely aligned to annotated
560 genes[56]. Differential gene expression analysis was then conducted using DESeq2 1.12.4 (betaPrior =
561 False) to normalize counts[60]. For each gene, a fold change in gene expression was defined as
562 $log_2 \frac{\text{Normalized count under food restriction (FR)}}{\text{Normalized count under control conditions (CTR)}}$ for males and females. Gene set enrichment analysis
563 (GSEA) was conducted using GSEA software (https://www.gsea-msigdb.org/gsea/index.jsp) using the
564 Hallmarks Gene Sets (v7.5.1).
565
566 **Statistics**

567 Statistical tests, p values, and the number and definition of independent units are stated in the figure
568 legends. For all measures, the number of animals was taken as the statically independent unit. Sample
569 size was determined by *a priori* based on calculations, with an aim of achieving 80% power on the
570 basis of a 20% group difference and a significance threshold of $p < 0.05$. Group means and variances
571 were taken from pilot data or previously published data[13]. Where applicable, ANOVA was used to
572 assess significance, followed by *post-hoc* Fisher LSD tests to prevent loss of power. Statistical tests
573 were carried out in Prism 6 (GraphPad Prism; RRID:SCR_002798). Averages denoted in figures
574 represent means, with error bars representing the standard error of the means (S.E.M.). We
575 complemented our statistical analyses using Bayes factor hypothesis testing (Supplemental Figure 1)
576 as described in[35,36] using JASP software to calculates Bayes factor, effect size, and confidence intervals
577 (https://jasp-stats.org/). As recommended, we used a default, Cauchy distribution with a spread of
578 $1/\sqrt{2}$ as a prior distribution of effect size. A $BF_{10} < 0.33$ is considered to be moderate evidence for the
579 absence of an effect[35,36].
580

581 ## Declaration of interests

582 The authors declare no competing interests.
583

584 ## References

585 1. Andersson B, Xu XF, Rebuffé-Scrive M, Terning K, Krotkiewski M, Björntorp P. The effects of
586 exercise, training on body composition and metabolism in men and women. *Int J Obes*.
587 1991;15(1):75-81.
588 2. Cortright RN, Koves TR. Sex Differences in Substrate Metabolism and Energy Homeostasis.
589 *Can J Appl Physiol*. 2000;25(4):288-311.
590 3. Volek J, Sharman M, Gómez A, et al. Comparison of energy-restricted very low-carbohydrate
591 and low-fat diets on weight loss and body composition in overweight men and women. *Nutr*
592 *Metab (Lond)*. 2004;1(1):13.
593 4. McCarthy D, Berg A. Weight Loss Strategies and the Risk of Skeletal Muscle Mass Loss.
594 *Nutrients*. 2021;13(7).
595 5. Tirosh A, De Souza RJ, Sacks F, Bray GA, Smith SR, LeBoff MS. Sex differences in the effects of
596 weight loss diets on bone mineral density and body composition: POUNDS LOST trial. *J Clin*
597 *Endocrinol Metab*. 2015;100(6):2463-2471.
598 6. Suchacki KJ, Thomas BJ, Ikushima YM, et al. The effects of caloric restriction on adipose tissue
599 and metabolic health are sex- and age-dependent. *Elife*. 2023;12.
600 7. Boutwell K, Rusch P. Some physiological effects associated with chronic caloric restriction. *Am*

601 *J Physiol*. 1948;154(3):517-524.
602 8. Ahlma RS, Prabakaran D, Mantzoros C, et al. Role of leptin in the neuroendocrine response to
603 fasting. *Nature*. 1996;382(6588):250-252.
604 9. Gill C, Rissman E. Female Sexual Behavior Is Inhibited by Short- and Long-term Food
605 Restriction. *Physiol Behav*. 1997;61(3):387-394.
606 10. Harris JJ, Jolivet R, Attwell D. Synaptic Energy Use and Supply. *Neuron*. 2012;75(5):762-777.
607 11. Attwell D, Laughlin SB. An Energy Budget for Signaling in the Grey Matter of the Brain. *J Cereb*
608 *Blood Flow Metab*. 2001;21(10):1133-1145.
609 12. Herculano-Houzel S. Scaling of Brain Metabolism with a Fixed Energy Budget per Neuron:
610 Implications for Neuronal Activity, Plasticity and Evolution. Perc M, ed. *PLoS One*.
611 2011;6(3):e17514.
612 13. Padamsey Z, Katsanevaki D, Dupuy N, Rochefort NL. Neocortex saves energy by reducing
613 coding precision during food scarcity. *Neuron*. 2022;110(2):280-296.e10.
614 14. Baile CA, Della-Fera MA, Martin RJ. Regulation of Metabolism and Body Fat Mass by Leptin.
615 *Annu Rev Nutr*. 2000;20(1):105-127.
616 15. Guo Z V, Hires SA, Li N, et al. Procedures for behavioral experiments in head-fixed mice. *PLoS*
617 *One*. 2014;9(2):e88678.
618 16. Goltstein PM, Reinert S, Glas A, Bonhoeffer T, Hübener M. Food and water restriction lead to
619 differential learning behaviors in a head-fixed two-choice visual discrimination task for mice.
620 *PLoS One*. 2018;13(9).
621 17. Toth LA, Gardiner TW. Food and Water Restriction Protocols: Physiological and Behavioral
622 Considerations. *Contemp Top Lab Anim Sci*. Published online 2000.
623 18. Burgess CR, Livneh Y, Ramesh RN, Andermann ML. Gating of visual processing by
624 physiological need. *Curr Opin Neurobiol*. 2018;49:16-23.
625 19. Burgess CR, Ramesh RN, Sugden AU, et al. Hunger-Dependent Enhancement of Food Cue
626 Responses in Mouse Postrhinal Cortex and Lateral Article Hunger-Dependent Enhancement
627 of Food Cue Responses in Mouse Postrhinal Cortex and Lateral Amygdala. *Neuron*.
628 2016;91(5):1154-1169.
629 20. Garza-Lombó C, Schroder A, Reyes-Reyes EM, Franco R. mTOR/AMPK signaling in the brain:
630 Cell metabolism, proteostasis and survival. *Curr Opin Toxicol*. 2018;8:102-110.
631 21. Dagon Y, Hur E, Zheng B, Wellenstein K, Cantley LC, Kahn BB. P70S6 kinase phosphorylates
632 AMPK on serine 491 to mediate leptin's effect on food intake. *Cell Metab*. 2012;16(1):104-
633 112.
634 22. Dagon Y, Avraham Y, Magen I, Gertler A, Ben-Hur T, Berry EM. Nutritional Status, Cognition,

and Survival. *J Biol Chem*. 2005;280(51):42142-42148.

23. Takei N, Nawa H. mTOR signaling and its roles in normal and abnormal brain development. *Front Mol Neurosci*. 2014;7(1 APR):1-12.

24. Herzig S, Shaw RJ. AMPK: Guardian of metabolism and mitochondrial homeostasis. *Nat Rev Mol Cell Biol*. 2018;19(2):121-135.

25. de la Cruz López KG, Toledo Guzmán ME, Sánchez EO, García Carrancá A. mTORC1 as a Regulator of Mitochondrial Functions and a Therapeutic Target in Cancer. *Front Oncol*. 2019;9(December):1-22.

26. Unger RH, Zhou YT, Orci L. Regulation of fatty acid homeostasis in cells: Novel role of leptin. *Proc Natl Acad Sci U S A*. 1999;96(5):2327-2332.

27. Poulsen L la C, Siersbæk M, Mandrup S. PPARs: Fatty acid sensors controlling metabolism. *Semin Cell Dev Biol*. 2012;23(6):631-639.

28. Wójtowicz S, Strosznajder AK, Jeżyna M, Strosznajder JB. The Novel Role of PPAR Alpha in the Brain: Promising Target in Therapy of Alzheimer's Disease and Other Neurodegenerative Disorders. *Neurochem Res*. 2020;45(5):972-988.

29. Kwon O, Kim KW, Kim MS. Leptin signalling pathways in hypothalamic neurons. *Cell Mol Life Sci*. 2016;73(7):1457-1477.

30. Brown LM, Clegg DJ. Central effects of estradiol in the regulation of food intake, body weight, and adiposity. *J Steroid Biochem Mol Biol*. 2010;122(1-3):65-73.

31. Estep PW, Warner JB, Bulyk ML. Short-Term Calorie Restriction in Male Mice Feminizes Gene Expression and Alters Key Regulators of Conserved Aging Regulatory Pathways. Orban L, ed. *PLoS One*. 2009;4(4):e5242.

32. Wood SH, Dam S van, Craig T, et al. Transcriptome analysis in calorie-restricted rats implicates epigenetic and post-translational mechanisms in neuroprotection and aging. *Genome Biol*. 2015;16(1):1-18.

33. Trevisiol A, Saab AS, Winkler U, et al. Monitoring ATP dynamics in electrically active white matter tracts. *Elife*. 2017;6.

34. Baeza-Lehnert F, Saab AS, Gutiérrez R, et al. Non-Canonical Control of Neuronal Energy Status by the Na + Pump. *Cell Metab*. 2019;29(3):668-680.e4.

35. van Doorn J, van den Bergh D, Böhm U, et al. The JASP guidelines for conducting and reporting a Bayesian analysis. *Psychon Bull Rev*. 2021;28(3):813-826.

36. Keysers C, Gazzola V, Wagenmakers EJ. Using Bayes factor hypothesis testing in neuroscience to establish evidence of absence. *Nat Neurosci*. 2020;23(7):788-799.

37. Collet TH, Sonoyama T, Henning E, et al. A metabolomic signature of acute caloric restriction.

669 *J Clin Endocrinol Metab*. 2017;102(12):4486-4495.
670 38. Cuevas-Cervera M, Perez-Montilla J, Gonzalez-Muñoz A, Garcia-Rios M, Navarro-Ledesma S.
671 The Effectiveness of Intermittent Fasting, Time Restricted Feeding, Caloric Restriction, a
672 Ketogenic Diet and the Mediterranean Diet as Part of the Treatment Plan to Improve Health
673 and Chronic Musculoskeletal Pain: A Systematic Review. *Int J Environ Res Public Health*.
674 2022;19(11):6698.
675 39. Hofer SJ, Carmona-Gutierrez D, Mueller MI, Madeo F. The ups and downs of caloric
676 restriction and fasting: from molecular effects to clinical application. *EMBO Mol Med*.
677 2022;14(1).
678 40. Mitchell SJ, Madrigal-Matute J, Scheibye-Knudsen M, et al. Effects of Sex, Strain, and Energy
679 Intake on Hallmarks of Aging in Mice. *Cell Metab*. 2016;23(6):1093-1112.
680 41. Kane AE, Sinclair DA, Mitchell JR, Mitchell SJ. Sex differences in the response to dietary
681 restriction in rodents. *Curr Opin Physiol*. 2018;6:28-34.
682 42. Gao Q, Horvath TL. Cross-talk between estrogen and leptin signaling in the hypothalamus. *Am*
683 *J Physiol - Endocrinol Metab*. 2008;294(5).
684 43. Irwin RW, Yao J, Hamilton RT, Cadenas E, Brinton RD, Nilsen J. Progesterone and estrogen
685 regulate oxidative metabolism in brain mitochondria. *Endocrinology*. 2008;149(6):3167-3175.
686 44. Brinton RD. Estrogen regulation of glucose metabolism and mitochondrial function:
687 Therapeutic implications for prevention of Alzheimer's disease. *Adv Drug Deliv Rev*.
688 2008;60(13-14):1504-1511.
689 45. Baar EL, Carbajal KA, Ong IM, Lamming DW. Sex- and tissue-specific changes in mTOR
690 signaling with age in C57BL/6J mice. *Aging Cell*. 2016;15(1):155-166.
691 46. Brown KD, Waggy ED, Nair S, et al. Sex Differences in Cardiac AMP-Activated Protein Kinase
692 Following Exhaustive Exercise. *Sport Med Int Open*. 2020;4(01):E13-E18.
693 47. Clemens AM, Lenschow C, Beed P, et al. Estrus-Cycle Regulation of Cortical Inhibition. *Curr*
694 *Biol*. 2019;29(4):605-615.e6.
695 48. Lin WC, Liu C, Kosillo P, et al. Transient food insecurity during the juvenile-adolescent period
696 affects adult weight, cognitive flexibility, and dopamine neurobiology. *Curr Biol*.
697 2022;32(17):3690-3703.e5.
698 49. de Carvalho T. Calorie restriction or dietary restriction: how far they can protect the brain
699 against neurodegenerative diseases? *Neural Regen Res*. 2022;17(8):1640.
700 50. Schroeder JE, Richardson JC, Virley DJ. Dietary manipulation and caloric restriction in the
701 development of mouse models relevant to neurological diseases. *Biochim Biophys Acta - Mol*
702 *Basis Dis*. 2010;1802(10):840-846.

703 51. Pakan JM, Lowe SC, Dylda E, et al. Behavioral-state modulation of inhibition is context-
704 dependent and cell type specific in mouse visual cortex. *Elife*. 2016;5:1-18.
705 52. Pakan JMP, Currie SP, Fischer L, Rochefort NL. The Impact of Visual Cues, Reward, and Motor
706 Feedback on the Representation of Behaviorally Relevant Spatial Locations in Primary Visual
707 Cortex. *Cell Rep*. 2018;24(10):2521-2528.
708 53. Henschke JU, Dylda E, Katsanevaki D, et al. Reward Association Enhances Stimulus-Specific
709 Representations in Primary Visual Cortex. *Curr Biol*. 2020;30(10):1866-1880.e5.
710 54. Kass RE, Raftery AE. Bayes Factors. *J Am Stat Assoc*. 1995;90(430):773-795.
711 55. Dobin A, Davis CA, Schlesinger F, et al. STAR: Ultrafast universal RNA-seq aligner.
712 *Bioinformatics*. 2013;29(1):15-21.
713 56. Liao Y, Smyth GK, Shi W. FeatureCounts: An efficient general purpose program for assigning
714 sequence reads to genomic features. *Bioinformatics*. 2014;30(7):923-930.
715

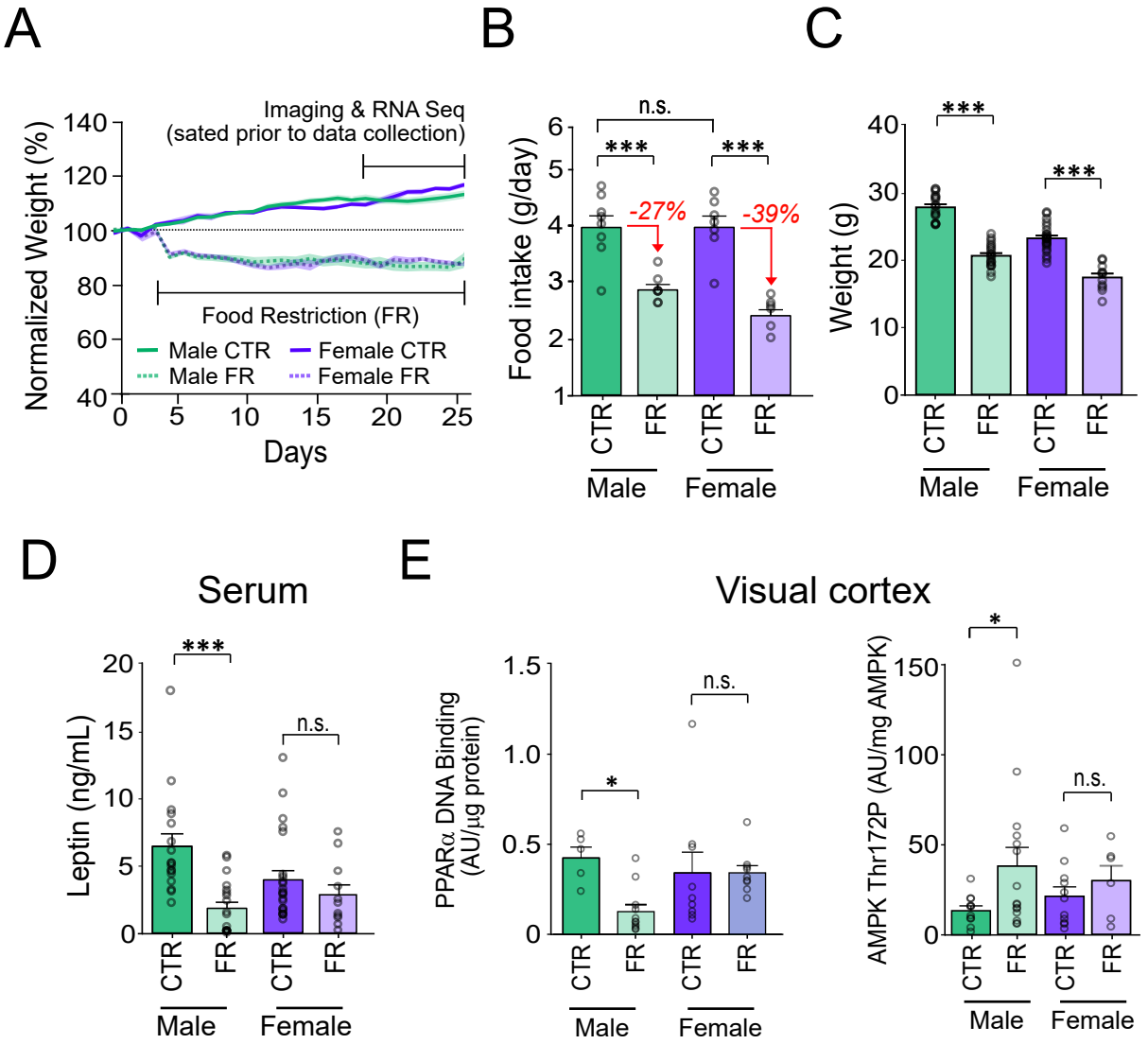
A
Imaging & RNA Seq
(sated prior to data collection)
Normalized Weight (%)
Food Restriction (FR)
Male CTR
Male FR
Female CTR
Female FR
Days
B
Food intake (g/day)
n.s.
***
***
-27%
-39%
CTR
FR
CTR
FR
Male
Female
C
Weight (g)
***
***
CTR
FR
CTR
FR
Male
Female
D
Serum
Leptin (ng/mL)
***
n.s.
CTR
FR
CTR
FR
Male
Female
E
Visual cortex
PPARα DNA Binding
(AU/μg protein)
*
n.s.
CTR
FR
CTR
FR
Male
Female
AMPK Thr172P (AU/mg AMPK)
*
n.s.
CTR
FR
CTR
FR
Male
Female

Figure 1

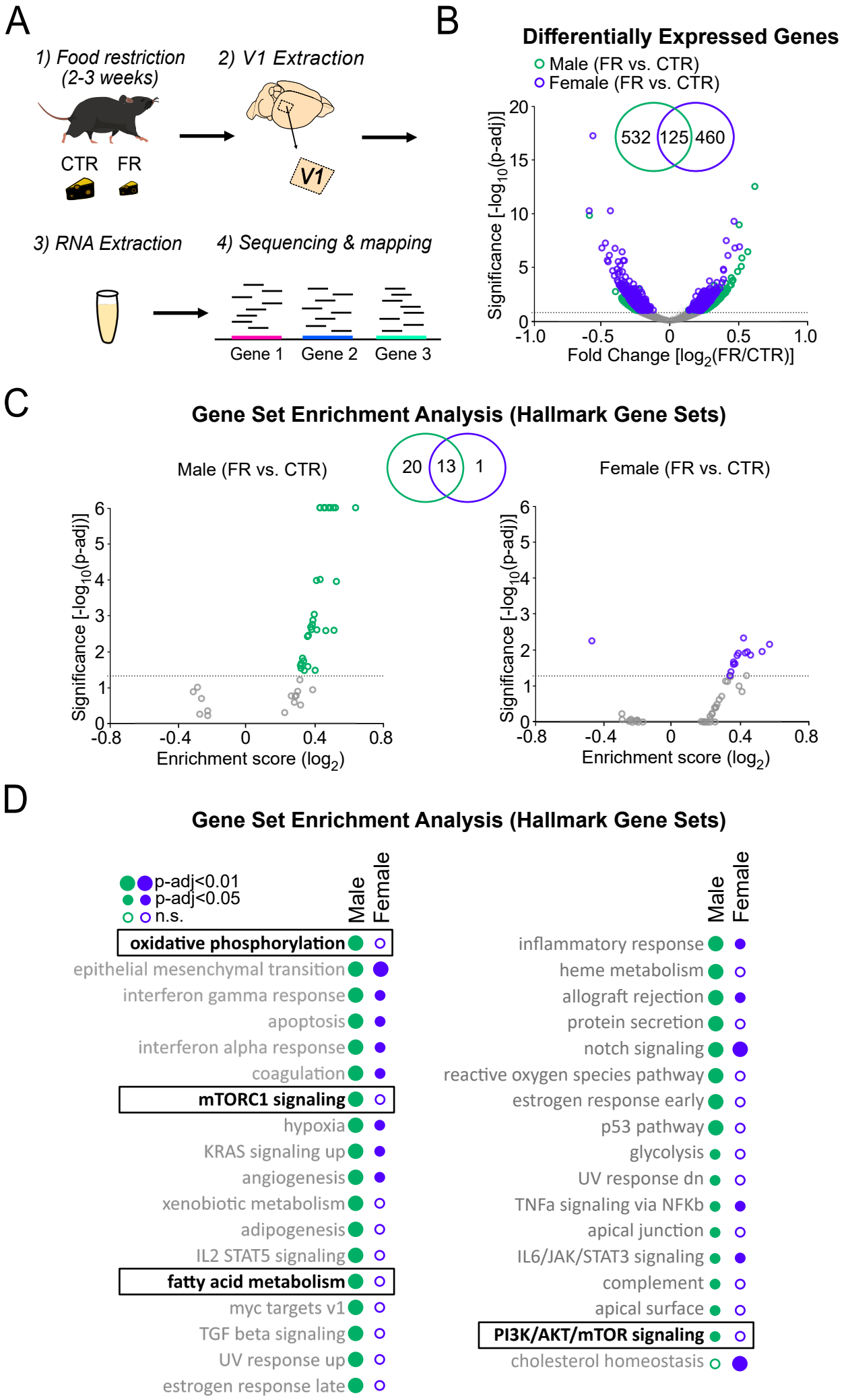
A
1) Food restriction (2-3 weeks)
2) V1 Extraction
CTR
FR
V1
3) RNA Extraction
4) Sequencing & mapping
Gene 1
Gene 2
Gene 3
B
Differentially Expressed Genes
Male (FR vs. CTR)
Female (FR vs. CTR)
532
125
460
Significance [-log10(p-adj)]
Fold Change [log2(FR/CTR)]
C
Gene Set Enrichment Analysis (Hallmark Gene Sets)
Male (FR vs. CTR)
20
13
1
Female (FR vs. CTR)
Significance [-log10(p-adj)]
Enrichment score (log2)
D
Gene Set Enrichment Analysis (Hallmark Gene Sets)
p-adj<0.01
p-adj<0.05
n.s.
Male
Female
oxidative phosphorylation
epithelial mesenchymal transition
interferon gamma response
apoptosis
interferon alpha response
coagulation
mTORC1 signaling
hypoxia
KRAS signaling up
angiogenesis
xenobiotic metabolism
adipogenesis
IL2 STAT5 signaling
fatty acid metabolism
myc targets v1
TGF beta signaling
UV response up
estrogen response late
inflammatory response
heme metabolism
allograft rejection
protein secretion
notch signaling
reactive oxygen species pathway
estrogen response early
p53 pathway
glycolysis
UV response dn
TNFa signaling via NFKb
apical junction
IL6/JAK/STAT3 signaling
complement
apical surface
PI3K/AKT/mTOR signaling
cholesterol homeostasis

Figure 2

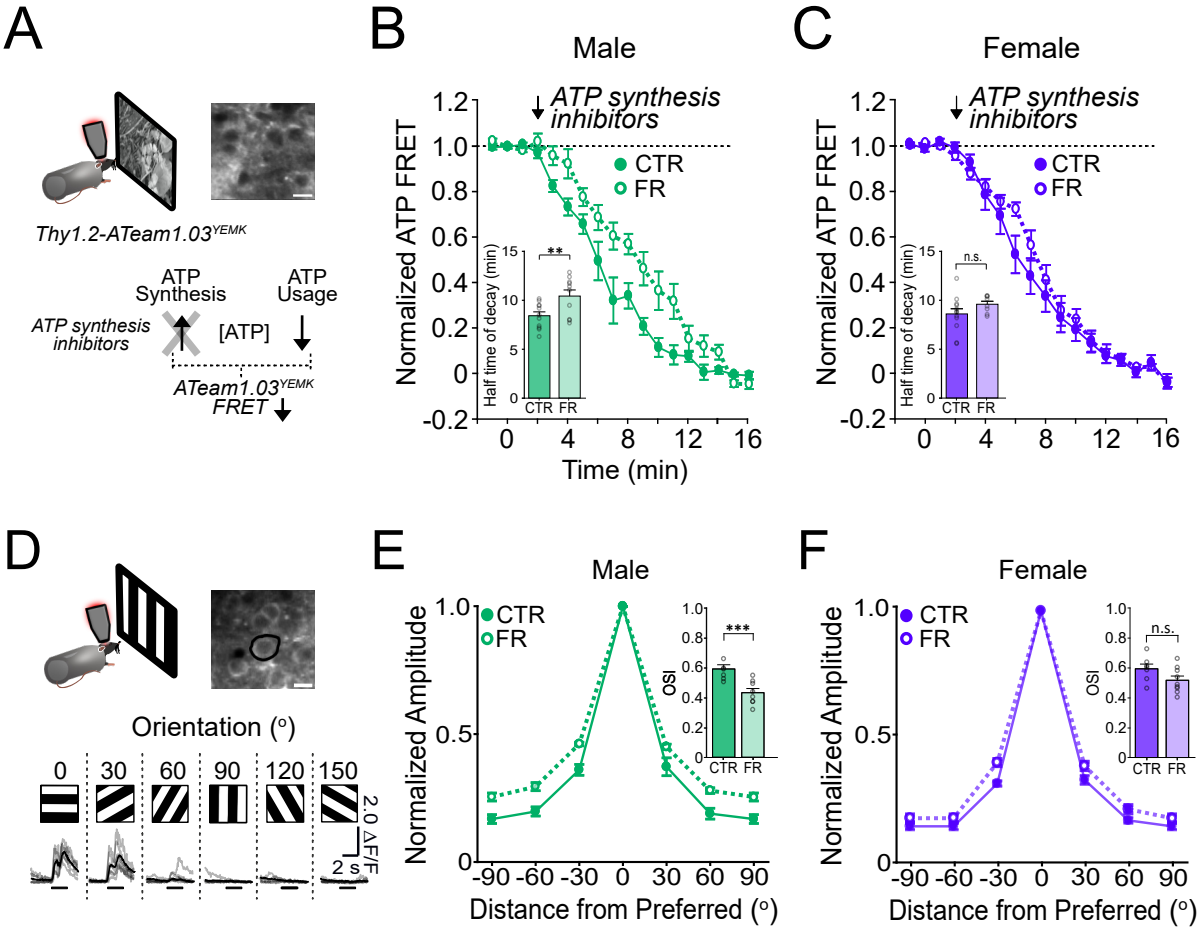
A
Thy1.2-ATeam1.03YEMK
ATP Synthesis
ATP Usage
ATP synthesis inhibitors
[ATP]
ATeam1.03YEMK FRET
B
Male
ATP synthesis inhibitors
CTR
FR
Normalized ATP FRET
Time (min)
Half time of decay (min)
**
C
Female
n.s.
D
Orientation (°)
0
30
60
90
120
150
2.0 ΔF/F
2 s
E
Male
Normalized Amplitude
Distance from Preferred (°)
OSI
***
F
Female

Figure 3

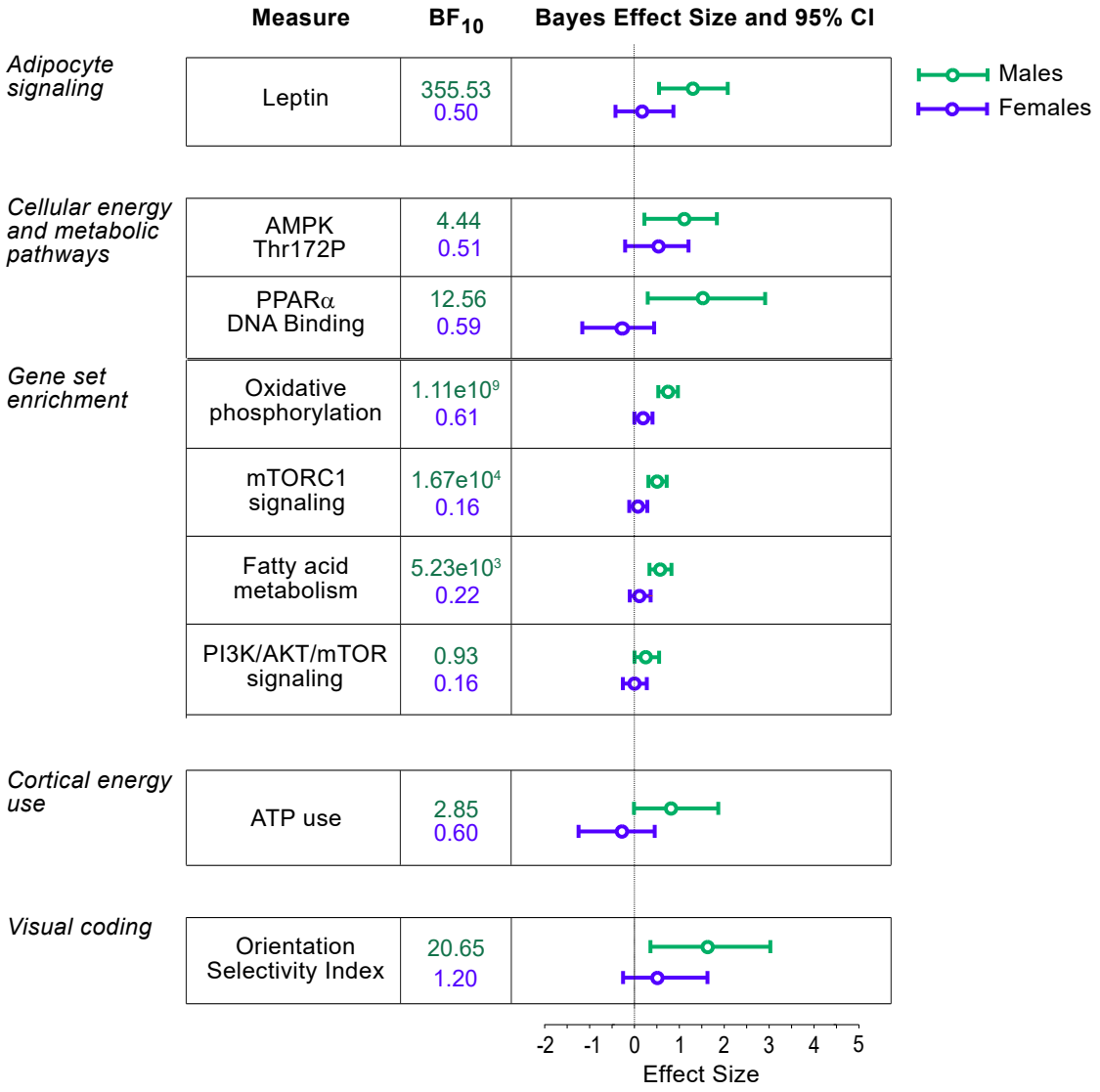
Measure
BF10
Bayes Effect Size and 95% CI
Adipocyte signaling
Leptin
355.53
0.50
Males
Females
Cellular energy and metabolic pathways
AMPK Thr172P
4.44
0.51
PPARα DNA Binding
12.56
0.59
Gene set enrichment
Oxidative phosphorylation
1.11e10^9
0.61
mTORC1 signaling
1.67e10^4
0.16
Fatty acid metabolism
5.23e10^3
0.22
PI3K/AKT/mTOR signaling
0.93
0.16
Cortical energy use
ATP use
2.85
0.60
Visual coding
Orientation Selectivity Index
20.65
1.20
-2 -1 0 1 2 3 4 5
Effect Size

Figure S1